Regional Studies in Marine Science 93 (2026) 104658

Contents lists available at ScienceDirect

Regional Studies in Marine Science

journal homepage: www.elsevier.com/locate/rsma

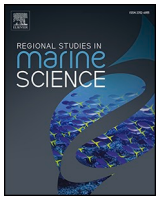

Genetic connectivity and regional differentiation of *Calanus sinicus* in Korean coastal wates with a focus on Yeosu Bay

Hyeongju Choi [a,b,1], Hyeongwoo Choi [c,1], Haeyoung Park [d], Seong-il Eyun [d,*], Ho Young Soh [a,b,**]

[a] Department of Environmental Oceanography, Chonnam National University, Yeosu 59626, Korea
[b] Department of Ocean Integrated Science, Chonnam National University, Yeosu 59626, Korea
[c] Department of Earth systems and Environmental Sciences, Chonnam National University, Gwangju 61186, Korea
[d] Department of Life Science, Chung-Ang University, Seoul 06974, Korea

ARTICLE INFO

Keywords:
Calanidae
Calanus sinicus
Yeosu Bay
Haplotype
ITS1
COX1

ABSTRACT

Calanus sinicus, an indicator species of the Yellow Sea cold bottom water, is generally abundant in Korean coastal waters, except in areas where summer environmental conditions are unfavorable. However, this species is notably dominant in Yeosu Bay (YB) along the south-central coast of Korea. This study aimed to provide a comprehensive analysis of the population genetic diversity, genetic structure, and haplotype network of *C. sinicus*, with a particular focus on investigating the origins of the YB population. To determine whether the *C. sinicus* YB population is indigenous or introduced, we collected samples from five regions: YB and four surrounding regions of the Korean peninsula (the eastern, southern, and western seas of Korea and the Yellow Sea). We amplified two genetic markers, the ribosomal *internal transcribed spacer 1* (*ITS1*, n = 155) and *cytochrome c oxidase subunit 1* (*COX1*, n = 117). To assess demographic patterns across the regions, Tajima's *D* and Fu and Li's *Fs* values were employed. YB population showed relatively low genetic diversity (π = 0.0034) and positive Tajima's *D* (1.07) and Fu and Li's *Fs* (1.13) values, indicating possible population contraction or balancing selection. YB also showed the greatest differentiation with the Ulleung Basin with N*st* and F*st* values of 0.03 respectively. Only *COX1* detected genetic distance based on the N*st* and F*st* values, highlighting its effectiveness in resolving regional genetic variation. However, haplotype minimum spanning networks for *COX1* showed no significant genetic isolation among the study regions, indicating substantial gene flow among *C. sinicus* populations. The strong genetic connectivity among *C. sinicus* populations suggests the presence of an oceanographic mechanism that facilitates the seasonal entry into YB during the summer.

1. Introduction

The copepod *Calanus sinicus* plays a significant ecological role in the marine ecosystems surrounding Korea, China, and Japan. It is particularly recognized as an indicator species of the subarctic cold-water layer of the Yellow Sea (Chen, 1964; Wang et al., 2014; Zhao et al., 2022). However, high summer water temperatures have adverse effects on *C. sinicus* populations (Pu et al., 2004; Zhang et al., 2007). Numerous studies has elucidated the temperature preferences of *C. sinicus*, showing that temperatures exceeding 26–27 °C lead to its disappearance (Huang and Chen, 1985; Lin and Chen, 1992; Jiaqi et al., 1997; Lin, 1997). Moreover, temperatures above 23 °C have been reported to induce stress in *C. sinicus* individuals (Uye, 1988) and the laboratory studies indicate that the adult mortality increases when the incubation temperature exceeds 23 °C (Huang and Zheng, 1986). Specifically, within the Northwest Pacific continental shelf ecosystem, *C. sinicus* plays a pivotal role in shaping species distributions. In the eastern Inland Sea of Japan and the adjacent Pacific Ocean, *C. sinicus* populations are predominantly concentrated in shelf waters, with densities decreasing both toward inshore and offshore areas (Uye, 2000). Its ecological significance is

* Corresponding author.
** Corresponding author at: Department of Environmental Oceanography, Chonnam National University, Yeosu 59626, Korea.
E-mail addresses: creo96326@jnu.ac.kr (H. Choi), creo9447@jnu.ac.kr (H. Choi), phy0328@cau.ac.kr (H. Park), eyun@cau.ac.kr (S.-i. Eyun), hysoh@chonnam.ac.kr (H.Y. Soh).
[1] These authors contributed equally to this work

https://doi.org/10.1016/j.rsma.2025.104658
Received 11 June 2025; Received in revised form 16 November 2025; Accepted 19 November 2025
Available online 21 November 2025
2352-4855/© 2025 The Authors. Published by Elsevier B.V. This is an open access article under the CC BY license (http://creativecommons.org/licenses/by/4.0/).

intriguing due to its limited access to the Chlorophyll-*a* rich, warm surface layers. This has led researchers to speculate that *C. sinicus* adopts a restricted diel vertical migration (DVM) (Wang et al., 2025) and utilization of the Yellow Sea cold bottom water (YSCBW) layer as a refuge, enabling individuals to avoid the warm surface waters during the day while ascending at night to feed (Pan et al., 2021). During the summer when coastal waters become warmer, *C. sinicus* population shift from the coast towards the central Yellow Sea. This movement is facilitated by the presence of the deep YSCBW, which serves as a thermal sanctuary, offering protection from the excessively warm surface temperatures (Wang et al., 2003).

Yeosu Bay (YB), located along the southern coast of Korea, is connected to Gwangyang Bay (a semi-enclosed water body to its north) through Yeosu Strait. The depth of Yeosu Strait ranges from 15 m to 40 m. During summer, the absence of distinct thermoclines, leads to vertical mixing and sea surface water temperature rises to 27–28 ℃ (Jeong et al., 2022). Due to its insufficient depth, YB is considered an unsuitable habitat for *C. sinicus*, as it lacks deep water refuges to escape the high temperatures during summer. However, *C. sinicus* has been observed in the area (Lee et al., 2017) and even dominates in Gwangyang Bay (Jang et al., 2004), despite challenging summer conditions for its survival.

To determine whether the *C. sinicus* population in Yeosu Bay is indigenous or introduced, and to assess its population connectivity with surrounding regions, we used the nuclear ribosomal internal transcribed spacer 1 (*ITS1*) and mitochondrial cytochrome *c* oxidase 1 (*COX1*) genes using specific primer pairs. The *COX1* gene is widely utilized for species identification across the animal kingdom (Hebert et al., 2003), notably in Crustacea (Costa et al., 2007) and various copepods (Bucklin and Lajeunesse, 1994; Bucklin et al., 2003; Jun et al., 2024).

In many species, mitochondrial genes evolve at a faster rate than nuclear genes. In copepods, for example, *Tigriopus californicus* exhibits an mtDNA synonymous site substitution rate that is approximately 55-fold higher than its nuclear DNA counterpart (Willett, 2012). Although life-history and habitat differences may limit direct generalization to *C. sinicus*, this case provides a more taxonomically relevant comparison than lice, suggesting that accelerated mtDNA evolution may operate among copepods more broadly. We included the *ITS1* gene as a nuclear marker because it has been shown to be effective for phylogenetic and population analyses in crustaceans (Chu et al., 2001), including copepods (Ki et al., 2009). In contrast to the mitochondrial *COX1* gene, which evolves rapidly and is widely used for intraspecific population studies, the nuclear *ITS1* provides complementary information and can offer deeper resolution of interspecific relationships across diverse animal groups.

This study aimed to provide a comprehensive analysis of the population genetic diversity, genetic structure, and haplotype network of *C. sinicus*, while also investigating the origins of *C. sinicus* populations in YB.

2. Materials and methods

2.1. Study area and collection

In this study, we conducted zooplankton sampling at different times across five coastal regions surrounding the Korean peninsula (Fig. 1, Tables 1 and 2): the Ulleung Basin (UB) in East Sea (July 2022), the northeastern East China Sea (NECS) (August 2023), YB in the northeastern East China Sea (October 2023), Gyeonggi Bay (GB) in the northern Yellow Sea (November 2023), and the southern Yellow Sea (SYS) (July 2024). To ensure the comparability of results, sampling procedures followed consistent protocols across all regions (see Supplementary Table S1 for more information).

Zooplankton were collected using different net types depending on the sampling site: a bongo net (net mouth diameter: 60 cm, mesh size: 200 μm) at NECS (depth: 75 m) and SYS (depth: 75 m); a conical net (net mouth diameter: 45 cm, mesh size: 200 μm) at YB (depth: 20 m) and GB (depth: 20 m); and a Multiple Opening/Closing Net and Environmental Sensing System (MOCNESS; net mouth area: 1 m^2, mesh size: 200 μm; Wiebe et al. 1985) at UB (depth: 60–30 m).

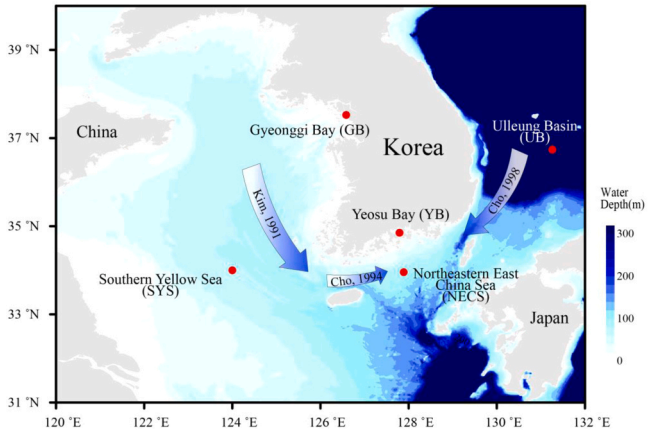

Fig. 1. Map of the study region and sampling sites for *Calanus sinicus* sampling. This study investigates five regions: the southern Yellow Sea (SYS) in the Yellow Sea of Korea, which is most influenced by the subarctic cold waters of the Yellow Sea; Gyeonggi Bay (GB), along the western of Korean coast; the northeastern East China Sea (NECS), in waters south of Korea; the Ulleung Basin (UB) in the East Sea/Sea of Japan, where the Kuroshio and East Korea Warm Currents intersect on the opposite side of the Korean peninsula from the Yellow Sea; and Yeosu Bay (YB) in southern Korea, the primary focus of this research.

The bongo and conical nets were towed vertically from stationary vessels without power, while the MOCNESS was towed obliquely through depth-stratified layers from a vessel proceeding at a speed of 1.0–1.5 knots. Despite using different net types, the consistent mesh size of 200 μm ensured that the sampling of adult females was not biased. Adult specimens of *C. sinicus* were identified under a stereomicroscope. This study focused exclusively on mature females, which were sorted under a stereomicroscope to ensure accurate identification and minimize potential sampling bias. The collected samples were immediately preserved in 95 % ethanol and transported to the laboratory.

2.2. DNA amplification and sequencing

DNA amplification and sequencing were employed not only for species identification but also to investigate population structure, haplotype diversity, and the origin of the *Calanus sinicus* population in Yeosu Bay. We extracted DNA using a 10 % Chelex solution following the protocols described in Casquet et al. (2012).

The concentration of extracted DNA was measured using a Qubit fluorometer, yielding 600 ng/μL. Due to the high concentration, the DNA was diluted 1:10 with distilled water, and 1 μL of the diluted DNA was used in each PCR reaction. Amplification reaction mixtures consisted of 17 μL of distilled water, 1 μL of diluted genomic DNA template, and 1 μL each of the forward and reverse primers (10 pmol each), giving a total reaction volume of 20 μL. The PCR premix included HotStart DNA Polymerase (1 U), dNTPs (250 μM each), and 1 × reaction buffer with 1.5 mM $MgCl_2$ (Bioneer, Korea).

Thermal cycling was carried out using either a Mastercycler (Eppendorf, Hamburg, Germany) or a MyGenie 96 Thermal Block (Bioneer, Daejeon, Korea). To optimize annealing temperatures, preliminary touchdown PCR tests were conducted, and the most distinct bands were obtained at 49.1 °C for *ITS1* and 48.9 °C for *COX1*, which were subsequently used in the main experiments. PCR reactions produced consistent results across both thermocyclers, demonstrating reproducibility. Standard precautions, including the use of a clean bench and filter tips, were followed to avoid contamination. The *ITS1* gene fragment was PCR-amplified using the primer pair forward *ITS1*

Table 1
Sample and molecular diversity statistics for *Calanus sinicus* based on the *ITS1* gene: *N* (number of samples), *n* (number of haplotypes), *h* (haplotype diversity), π (nucleotide diversity), *D* (Tajima's *D*), *Fs* (Fu and Li's *Fs*). Statistical significance is represented by asterisks: *, $p < 0.05$; **, $p < 0.005$; and ***, $p < 0.001$.

Locality	Station	Latitude	Longitude	*ITS1*					
				N	***n***	***h***	***π***	***D***	***Fs***
Northeastern East China sea	Yeosu Bay (YB)	34° 51' 06''	127° 47' 35''	25	2	0.08	NA	−1.16	−1.72
East Sea	Ulleung Basin (UB)	36° 45' 26''	131° 15' 55''	21	6	0.43	NA	−2.06*	−3.18**
Northeastern East China sea	Northeastern East China Sea (NECS)	33° 57' 25''	127° 53' 17''	62	7	0.19	0.003	−2.85***	−6.18**
Western of Korean waters	Gyeonggi Bay (GB)	37° 31' 30''	126° 23' 35''	31	1	NA	NA	NA	NA
Southern Yellow Sea	Southern Yellow Sea (SYS)	34°	124°	16	3	0.24	NA	−1.5	−1.91
Total				155	13	0.15	0.001	−2.86***	−9.5**

Table 2
Sample and molecular diversity statistics for *Calanus sinicus* based on the *COX1* gene: *N* (number of samples), *n* (number of haplotypes), *h* (haplotype diversity), π (nucleotide diversity), *D* (Tajima's *D*), *Fs* (Fu and Li's *Fs*). Statistical significance is represented by asterisks: *, $p < 0.05$; **, $p < 0.005$; and ***, $p < 0.001$.

Locality	Station	Latitude	Longitude	*COX1*					
				N	***n***	***h***	***π***	***D***	***Fs***
Northeastern East China sea	Yeosu Bay (YB)	34° 51' 06''	127° 47' 35''	12	6	0.8	0.003	1.07	1.13
East Sea	Ulleung Basin (UB)	36° 45' 26''	131° 15' 55''	19	18	0.99	0.008	−1.76	−2.79*
Northeastern East China sea	Northeastern East China Sea (NECS)	33° 57' 25''	127° 53' 17''	25	13	0.94	0.007	−1.37	−2.35
Western of Korean waters	Gyeonggi Bay (GB)	37° 31' 30''	126° 23' 35''	26	15	0.94	0.007	−1.84*	−3.55**
Southern Yellow Sea	Southern Yellow Sea (SYS)	34°	124°	35	8	0.72	0.003	−0.86	−2.15
	Total			117	37	0.89	0.006	−2.36**	−6.21**

(TCCGTAGGTGAACCTGCGG) primer and reverse *ITS4* (TCCTCCGCTTATTGATATGC) primers (Vilgalys, 1994; Estoup et al., 1996; Kumar and Shukla, 2005).

The thermal cycling protocol included an initial denaturation step at 95 ℃ for 3 min, followed by 35 cycles of denaturation at 95 ℃ for 30 s, annealing at 49.1 ℃ for 30 s, and elongation at 72 ℃ for 1 min, with a final extension step at 72 ℃ for 7 min. The mitochondrial *COX1* gene was amplified using the primer pair forward LCO1490 (GGTCAACAAATCATAAAGATATTGG) and reverse HCO2198 (TAAACTTCAGGGTGACCAAAAAATCA) primers (Folmer et al., 1994). The thermal cycling protocol consisted of an initial denaturation step at 95 ℃ for 3 min, followed by 35 cycles of denaturation at 95 ℃ for 30 s, annealing at 48.9 ℃ for 30 s, and elongation at 72 ℃ for 1 min, with a final 7-minute extension step at 72 ℃. The PCR products were electrophoresed in a 1 % Tris acetate-EDTA agarose gel at 100 V for 20 min with a 100 bp DNA ladder. Subsequently, PCR products exhibiting positive results were subjected to purification and sequencing at Macrogen (Daejeon, Korea). The *COX1* and *ITS1* haplotype sequences used in this study, are publicly available in the National Center for Biotechnology Information (NCBI) GenBank under the accession numbers PQ524704–PQ524820 and PQ535719–PQ535873, respectively.

2.3. Population dynamics

A total of 117 sequences were aligned for *COX1*, covering 480 base pairs in length, while 155 sequences were aligned for *ITS1*, spanning 709 base pairs. The DNA sequences were aligned using mafft (ver. 7.505) with the default parameters to identify highly conserved regions within each gene set (Katoh et al., 2002). Haplotypes were determined using DnaSP (ver. 6.12) (Rozas et al., 2017), a software designed for comprehensive DNA sequence variation. DnaSP was also employed to calculate general statistical indices, including haplotype diversity (*h*) and nucleotide diversity (π). Furthermore, Tajima's *D* (Tajima 1989) and Fu and Li's *Fs* (Fu 1997) neutrality statistics were examined to assess population dynamics and potential deviations. Negative values of Tajima's *D* ($D < 0$) or Fu and Li's *Fs* suggest population expansion, while positive values of *D* ($D > 0$) may indicate population contraction, potentially due to a recent bottleneck. Moreover, a negative *D* may also imply purifying selection, whereas a positive *D* could suggest the prevalence of overdominant selection in the region. To further assess genetic differentiation, we computed the fixation index (F*st*) using 1000 permutations and examined pairwise genetic divergence among populations by DnaSP. The standard F*st* scale was adopted for this analysis, providing a quantitative measure of genetic variance and gene flow (Barbosa et al., 2019): F*st* values below 0 were regarded as 0, little genetic divergence was inferred for F*st* values between 0 and 0.05, moderate genetic divergence was inferred for F*st* values between 0.05 and 0.15, significant genetic divergence was inferred for F*st* values between 0.15 and 0.25, and substantial genetic divergence was indicated by F*st* values exceeding 0.25.

2.4. Population structure analysis

To determine the best nucleotide evolutionary models for the *ITS1* and *COX1* genes, we employed ModelFinder as implemented in IQ-TREE (ver. 2.2.0.3) (Kalyaanamoorthy et al., 2017). A maximum likelihood (ML) tree was reconstructed using RAxML-NG (ver. 0.9.0) with "GTR + F + I + G4" substitution model for both *COX1* and *ITS1* genes (Kozlov et al., 2018). Finally, haplotype networks of *ITS1* and *COX1* genes were generated using PopArt (ver. 1.7) via the median-joining method (Leigh et al., 2015).

3. Results

3.1. C. sinicus YB population

The nuclear ribosomal *ITS1* genes were sequenced from 155 *C. sinicus* individuals collected from five regions surrounding the Korean peninsula: YB, SYS, GB, NECS, and UB. A total of 13 *ITS1* haplotypes were identified (Table 1). Among the sampled sites, UB exhibited the highest haplotype diversity ($h = 0.43$), while YB showed the lowest ($h = 0.08$). Nucleotide diversity was highest in NECS ($\pi = 0.0036$) and lowest in YB ($\pi = 0.0001$). In GB, both haplotype and nucleotide diversity were zero, as only a single haplotype was detected. Across all regions, Tajima's *D* and Fu and Li's *Fs* values were negative, suggesting potential population expansion or purifying selection.

Mitochondrial *COX1* gene fragments (600 bp) were sequenced from 117 *C. sinicus* individuals collected from the same five regions. From this dataset, 37 *COX1* haplotypes were identified (Table 2). Haplotype diversity was highest in UB ($h = 0.99$), and nucleotide diversity was also

highest in UB ($\pi = 0.0077$). Conversely, the lowest haplotype ($h = 0.72$) and nucleotide ($\pi = 0.003$) diversities were observed in SYS. Tajima's *D* and Fu's *Fs* values were negative across all regions, except for YB.

Compared to *ITS1*, *COX1* exhibited higher haplotype diversity ($h = 0.89$ vs. $h = 0.15$) and nucleotide diversity ($\pi = 0.006$ vs. $\pi = 0.0016$) across all populations.

3.2. Genetic connectivity

Across five different regions, we identified 37 *COX1* haplotypes from 117 *C. sinicus* individuals and 13 *ITS1* haplotypes from 155 individuals. To analyze genetic relationships and relative frequencies of these haplotypes, we utilized a minimum spanning network. This approach provided a clear visualization of haplotype connectivity and potential lineage divergence among populations.

The network analysis of the *COX1* haplotypes identified three major haplogroups (Hap_1, Hap_2, and Hap_3) that were shared across all five regions (Fig. 2a). Hap_5 and Hap_6 were common to four regions (GB, SYS, NECS, and UB), while Hap_10 was present in three regions (GB, NECS, and UB). Hap_4 (YB and UB), Hap_12 (NECS and UB), and Hap_19 (SYS and UB) were shared between two regions. All remaining haplotypes were site-specific, with no unique haplotypes found in YB (Fig. 2a). Among the three primary haplotypes (Hap_1, Hap_2, and Hap_3), Hap_1 comprised of 13 individuals, with 8.33 % from YB, 14.29 % from SYS, 8 % from NECS, 5.26 % from UB, and 15.38 % from GB. Hap_2 were the most prevalent, comprising 31 individuals, with 4.67 % from YB, 45.71 % from SYS, 16 % from NECS, 5.26 % from UB, and 19.23 % from GB. Hap_3 included 18 individuals, with 25 % from YB, 25.71 % from SYS, 16 % from NECS, 5.26 % from UB, and 3.85 % from GB.

In contrast to the *COX1*, the *ITS1* network showed a single clade, with the majority of individuals belonging to one dominant haplotype (Hap_1). The remaining haplotypes were singletons. Hap_1 comprised of 143 individuals, accounting for 100 % of the YB and GB populations, 93.75 % of the NECS, 90.32 % of the SYS, and 76.19 % of the UB individuals. This pattern indicates limited genetic differentiation in *ITS1* across the sampled regions, suggesting a high level of genetic connectivity among *C. sinicus* populations.

3.3. Genetic differentiation

We analyzed the distribution of three primary haplotypes (Hap_1, Hap_2, and Hap_3) across the five regions (Fig. 3). Hap_2 was the most dominant in SYS, representing 45.7 % of individuals, followed by YB (41.7 %), GB (19.2 %), NECS (16 %), and UB (5.3 %). Hap_3 was also the most frequency in SYS, with 25.7 %, followed by YB (25 %), NECS (16 %), UB (5.3 %), and GB (3.85 %). Hap_1 was most common in GB (15.4 %), followed by SYS (14.3 %), YB (8.3 %), NECS (8 %), and UB (5.3 %). The number of unique haplotypes per region ranged from 4 to 9, except for YB, which had none (Fig. 3).

Pairwise genetic distance analysis showed that N*st* and F*st* values for

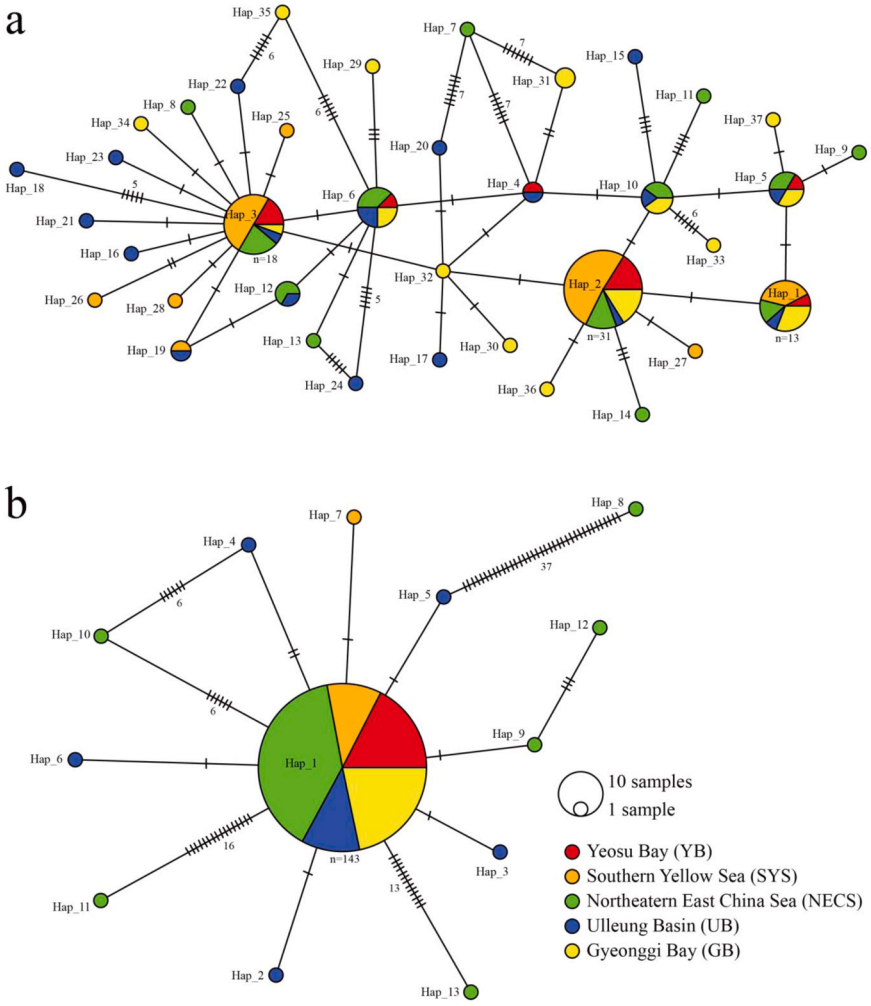

Fig. 2. ***Calanus sinicus*** **haplotype network analysis based on two genes: (a) 37** ***COX1*** **haplotypes and (b) 155** ***ITS1*** **haplotypes**. The haplotype network was constructed using median-joining method. Colors represent the sampling locations, and each circle represents one allele, and lines indicate lineage. Circle size is proportional to the frequency of the haplotype. The crossbars on each branch indicate the mutation steps.

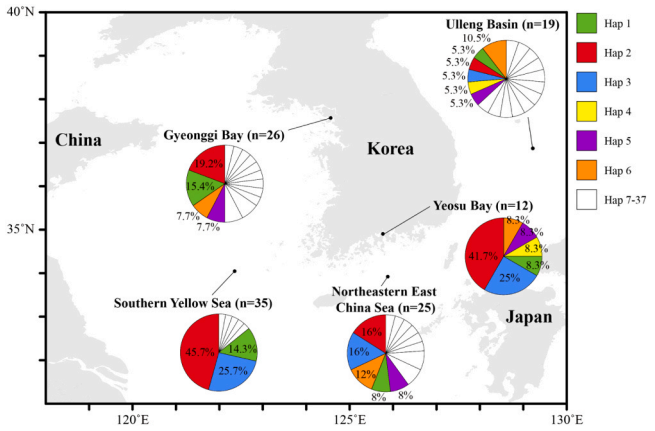

Fig. 3. Geographic distribution of *Calanus sinicus* haplotypes based on *COX1*. Due to the inability to represent all haplotypes with distinct colors, only the haplotypes present in Yeosu Bay or with a frequency exceeding 5 % are displayed.

ITS1 ranged from 0 to 0.004 across all regions (Table 3). In contrast, F*st* values based on *COX1* varied from 0 to 0.097, with the highest genetic differentiation observed between UB–SYS (Table 4). Additionally, moderate genetic differentiation was identified for SYS–NECS (0.088), SYS–GB (0.061), and GB–UB (0.051). For all other regions, F*st* values remained below 0.05, indicating minimal genetic differentiation.

4. Discussion

4.1. Genetic differentiation

In our study, we analyzed nucleotide sequence variations to assess intraspecies differences. Species identification based on ribosomal *ITS1* and mitochondrial *COX1* genes consistently confirmed *C. sinicus*, supporting our morphological identifications. The rate of nucleotide substitution varies between mtDNA and nuclear DNA across different organisms. Previous studies have shown that the *ITS1* gene is a reliable marker for phylogenetic and clustering analyses in crustaceans (Chu et al., 2001) and copepods (Elvers et al., 2006; Ki et al., 2009), while the *COX1* gene has been widely used for species identification in crustaceans (Quan et al., 2001; Väinölä et al., 2001), particularly copepods (Burton and Lee, 1994; Edmands, 2001; Eyun et al., 2007; Eyun, 2017; Song et al., 2021; Song et al., 2024; Choi et al., 2025).

However, in this study, the *ITS1* gene failed to effectively distinguish intraspecies variation whereas *COX1* gene successfully captured these differences. This finding aligns with previous research suggesting that mtDNA evolves more rapidly than nuclear DNA (Johnson et al., 2003). The ability of *COX1* to detect both interspecies differences and genetic variability underscores its value in molecular analyses of copepods. Given the significant differences observed using a single mitochondrial marker, future studies should incorporate additional mitochondrial genes to further refine genetic differentiation analyses.

Table 3
Pairwise N*st* and F*st* values based on *ITS1* for pairwise comparisons between *Calanus sinicus* populations in Korean seas. The N*st* values are above the diagonal, and F*st* values are below the diagonal. According to Barbosa et al. (2019), F*st* < 0.05 reflects little genetic differentiation, while 0.05 < F*st* < 0.15 indicates moderate divergence.

Station	Yeosu Bay	Southern Yellow Sea	Ulleung Basin	Northeastern East China Sea	Gyeonggi Bay
Yeosu Bay	-	0	0	0.004	0
Southern Yellow Sea	0	-	0	0.004	0
Ulleung Basin	0	0	-	0.001	0
Northeastern East China Sea	0.004	0.004	0.001	-	0.004
Gyeonggi Bay	0	0	0	0.004	-

Table 4
Pairwise N*st* and F*st* values based on *COX1* for pairwise comparisons between *Calanus sinicus* populations in Korean seas. The N*st* values are above the diagonal, and F*st* values are below the diagonal. According to Barbosa et al. (2019), F*st* < 0.05 reflects little genetic differentiation, while 0.05 < F*st* < 0.15 indicates moderate divergence.

Station	Yeosu Bay	Southern Yellow Sea	Ulleung Basin	Northeastern East China Sea	Gyeonggi Bay
Yeosu Bay	-	0	0.03	0	0
Southern Yellow Sea	0	-	0.097	0.088	0.061
Ulleung Basin	0.03	0.097	-	0.004	0.051
Northeastern East China Sea	0	0.088	0.004	-	0
Gyeonggi Bay	0	0.061	0.051	0	-

4.2. Connectivity of C. sinicus populations around the Korean peninsula

Analysis of genetic distances using the *COX1* gene revealed a significant difference between the SYS and UB sites, with an F*st* value of 0.097 (Table 4). A key finding of the study was that while YB displayed low genetic differentiation from UB (F*st* = 0.03, Table 3), it showed no discernible difference from SYS (F*st* = 0, Table 3). Previous studies have shown that the cold bottom water from the Yellow Sea flows southward along the northern section of the Jeju Strait (Kim et al., 1991; Kang and Moon, 2022) before entering the South Sea (Cho and Kim, 1994). This suggest that the primary influence on the YB population comes from the SYS, as evidenced by its genetic similarity to UB and GB populations. These findings strongly indicate that the *C. sinicus* population in YB probably originated from the SYS. However, given the shared genetic components between YB and UB haplotypes, some influence from the UB cannot be ruled out entirely (Fig. 2a).

During past glacial periods, a significant decline in sea level exceeding 120 m exposed the continental shelf surrounding the Korean peninsula (Lee et al., 2008). Following the Last Glacial Maximum, the gradual rise in sea level modified regional oceanographic conditions, particularly within the Korea Strait (Lee et al., 2021). These hydrodynamic changes likely played a role in shaping the ecological characteristics of the seas surrounding the Korean peninsula. However, due to extensive gene flow, population differentiation was not detected in this study. Furthermore, the high levels of genetic exchange observed in this study highlight the role of ocean currents in shaping copepod populations. As zooplankton, *C. sinicus* individuals are highly influenced by water movement, emphasizing the need to consider oceanographic factors when studying their population dynamics.

The F*st* value for NECS–SYS was 0.088, whereas NECS–UB was 0.004 (Table 3), indicating a closer genetic relationship between NECS and SYS than between NECS and UB. Based on the *COX1* gene, UB had the highest haplotype diversity (0.99) among the four regions (Table 2). High haplotype diversity in an introduced population often suggests multiple introductions from several donor regions (Voisin et al., 2005). The unique sharing of haplotypes between NECS and UB suggests putative genetic exchange between these two regions (Fig. 2a), possibly influenced by the Tsushima Warm Current (Yoon and Yoon, 2015) and the summer circulation of the Korea Strait Coastal Branching Water (Cho and Kim, 1998).

Additionally, previous studies have reported the southward expansion of Korean Sea Bottom Cold Water during the summer, followed by its return to the UB (Cho and Kim, 1998). A comparison of YB haplotypes

with those from both UB and SYS further highlights the substantial influence of the SYS on YB population.

4.3. *C. sinicus* YB population

In YB, *C. sinicus* populations dominate despite the challenging summer conditions including shallow depths and lack of distinct thermoclines. Unlike the central region of the Yellow Sea, YB lacks refuges with temperatures below 10℃ during summer. In our experiment, we used *COX1* and *ITS1* genes to confirm population expansion or decline based on Tajima's *D* and Fu and Li's *Fs* statistics. Negative *D* and *Fs* values indicate population expansion, while positive values suggest contraction. Negative values were observed at GB (*COX1*: $D = -1.84$, $Fs = -3.55$ and *ITS1*: $D = 0$, $Fs = 0$), SYS (*COX1*: $D = -0.86$, $Fs = -2.15$ and *ITS1*: $D = 1.5$, $Fs = -1.91$), NECS (*COX1*: $D = -1.37$, $Fs = -2.35$ and *ITS1*: $D = -2.85$, $Fs = -6.18$), and UB (*COX1*: $D = -1.76$, $Fs = -2.79$ and *ITS1*: $D = -2.06$, $Fs = -3.18$) (Tables 1 and 2). However, YB showed positive values (*COX1*: $D = 1.07$, and $Fs = 1.13$ (Table 2) suggesting unfavorable conditions for *C. sinicus* in YB compared to other regions due to a recent bottleneck (Gattepaille et al., 2013; Puvanasundram et al., 2018). Despite the low temperature and limited food availability, YSCBW serves as a summer refuge for *C. sinicus*, allowing them to evade high surface temperatures, albeit with reduced growth rates at copepodite stage 5 (Li et al., 2004; Pu et al., 2004). In our own measurements conducted in YB during the summer of 2023, the lower layer temperature ranged from 24.7 to 29 °C, while the surface temperature ranged from 26 to 28.5 °C. Considering the elevated summer temperatures in YB, copepodite stage 5 of *C. sinicus* remains in an unfavorable environment without a resting refuge. Nevertheless, the persistent occurrence of *C. sinicus* in YB raises questions about their survival strategies. If *C. sinicus* continues to appear in YB during summer, this may indicate local adaptation or the presence of an independent population, and further investigations are needed to elucidate the mechanisms by which the YB population tolerates elevated summer surface temperatures. To further elucidate the population structure and evolutionary dynamics of the *C. sinicus* species, future studies should incorporate multi-marker genetic analyses, including both mitochondrial and nuclear markers, to provide a more comprehensive view of genetic diversity and gene flow. Additionally, integrating ocean current modeling would help clarify the influence of physical dispersal barriers and connectivity patterns on population distribution. Longer temporal sampling across multiple seasons or years is also recommended to capture temporal genetic variation and potential shifts in population dynamics due to environmental changes.

5. Conclusion

The mitochondrial *COX1* gene proved to be a more effective marker for genetic divergence within *C. sinicus* compared to the nuclear *ITS1* gene. Additionally, *COX1* showed negative values in four regions, with YB showing positive values indicating population contraction due to a recent bottleneck effect. These findings indicate that *C. sinicus* in YB faces significant environmental pressures during the summer. Also, YB showed the greatest F*st* and N*st* values (0.03) with UB while no discernible differences were found in SYS. Based on the markers used, the genetic evidence is most consistent with influence from southwestern Korea on the *C. sinicus* population in YB, rather than with an origin in the East Sea of Korea.

Ethical approval

Not applicable.

Funding

This work was supported by Korea Institute of Marine Science & Technology Promotion funded by the Ministry of Oceans and Fisheries, Korea (RS-2018-KS181192 and RS-2025–02215227) and the Chung-Ang University Research Scholarship Grants in 2025.

CRediT authorship contribution statement

Hyeongju Choi: Writing – original draft, Writing – review & editing, Resources, Methodology, Investigation, Formal analysis. **Hyeongwoo Choi:** Writing – original draft, Writing – review & editing, Methodology, Investigation, Formal analysis. **Haeyoung Park:** Visualization, Data curation. **Seong-il Eyun:** Writing – review & editing, Supervision, Project administration. **Ho Young Soh:** Conceptualization, Writing – review & editing, Supervision, Project administration.

Declaration of Competing Interest

The authors declare that they have no known competing financial interests or personal relationships that could have appeared to influence the work reported in this paper.

Appendix A. Supporting information

Supplementary data associated with this article can be found in the online version at doi:10.1016/j.rsma.2025.104658.

Data availability

I have uploaded raw data to the NCBI

References

Barbosa, C., Trevisan, R., Estevinho, T.F., Castellani, T.T., Silva-Pereira, V., 2019. Multiple introductions and efficient ropagule dispersion can lead to high genetic variability in an invasive clonal species. Biol. Invasions 21, 3427–3438. https://doi.org/10.1007/s10530-019-02057-y.

Bucklin, A., Frost, B., Bradford-Grieve, J., Allen, L., Copley, N., 2003. Molecular systematic and phylogenetic assessment of 34 calanoid copepod species of the Calanidae and Clausocalanidae. Mar. Biol. 142, 333–343. https://doi.org/10.1007/s00227-002-0943-1.

Bucklin, A., Lajeunesse, T.C., 1994. Molecular genetic variation of *Calanus pacificus* (Copepoda: Calanoida): preliminary evaluation of genetic structure and subspecific differentiation based on mtDNA sequences. CalCOFi 35, 45–51.

Burton, R.S., Lee, B.N., 1994. Nuclear and mitochondrial gene genealogies and allozyme polymorphism across a major phylogeographic break in the copepod *Tigriopus californicus*. Proc. Natl. Acad. Sci. USA 91, 5197–5201. https://doi.org/10.1073/pnas.91.11.5197.

Casquet, J., Thebaud, C., Gillespie, R.G., 2012. Chelex without boiling, a rapid and easy technique to obtain stable amplifiable DNA from small amounts of ethanol-stored spiders. Mol. Ecol. Resour. 12, 136–141. https://doi.org/10.1111/j.1755-0998.2011.03073.x.

Chen, Q., 1964. A study of the reproduction, variation in sex ratio and variation in size of *Calanus sinicus*. Oceanol. Limnol. Sin. 6, 272–288.

Cho, Y.K., Kim, K., 1994. Characteristics and origin of the cold water in the South Sea of Korea in summer. KSO 29, 414–421.

Cho, Y.K., Kim, K., 1998. Structure of the Korea Strait Bottom Cold Water and its seasonal variation in 1991. Cont. Shelf Res. 18, 791–804.

Choi, H., Yu, O., Eyun, S., 2025. Evolutionary insights into adaptation of hemocyanins from deep-sea hydrothermal vent shrimps. Mar. Pollut. Bull. 215, 117872. https://doi.org/10.1016/j.marpolbul.2025.117872.

Chu, K.H., Li, C.P., Ho, H.Y., 2001. The first internal transcribed spacer (*ITS-1*) of ribosomal DNA as a molecular marker for phylogenetic and population analyses in Crustacea. Mar. Biotechnol. 3, 355–361. https://doi.org/10.1007/s10126001-0014-5.

Costa, F.O., Dewaard, J.R., Boutillier, J., Ratnasingham, S., Dooh, R.T., Hajibabaei, M., Hebert, P.D., 2007. Biological identifications through DNA barcodes: the case of the Crustacea. Can. J. Fish. Aquat. Sci. 64, 272–295. https://doi.org/10.1139/f07-008.

Edmands, S., 2001. Phylogeography of the intertidal copepod *Tigriopus californicus* reveals substantially reduced population differentiation at northern latitudes. Mol. Ecol. 10, 1743–1750. https://doi.org/10.1046/j.0962-1083.2001.01306.x.

Elvers, D., Böttger, S.R., Blohm, D., Hagen, W., 2006. Sympatric size variants of the microcopepod Oncaea venusta exhibit distinct lineages in DNA sequences. Mar. Biol. 149, 503–513. https://doi.org/10.1007/s00227-005-0234-8.

Estoup, A., Largiader, C.R., Perrot, E., Chourrout, D., 1996. Rapid one-tube DNA extraction for reliable PCR detection of fish polymorphic markers and transgenes. Mol. Mar. Biol. Biotechnol. 5, 295–298.

Eyun, S., 2017. Phylogenomic analysis of Copepoda (Arthropoda, Crustacea) reveals unexpected similarities with earlier proposed morphological phylogenies. BMC Evol. Biol. 17, 23. https://doi.org/10.1186/s12862-017-0883-5.
Eyun, S., Lee, Y., Suh, H., Kim, S., Soh, H.Y., 2007. Genetic identification and molecular phylogeny of *Pseudodiaptomus* species (Calanoida, Pseudodiaptomidae) in Korean waters. Zool. Sci. 24, 265–271.
Folmer, O., Black, M., Hoeh, W., Lutz, R., Vrijenhoek, R., 1994. DNA primers for amplification of mitochondrial *cytochrome c oxidase subunit I* from diverse metazoan invertebrates. Mol. Mar. Biol. Biotechnol. 294–299.
Gattepaille, L.M., Jakobsson, M., Blum, M.G.B., 2013. Inferring population size changes with sequence and SNP data: lessons from human bottlenecks. Hered 110, 409–419. https://doi.org/10.1038/hdy.2012.120.
Hebert, P.D., Cywinska, A., Ball, S.L., Dewaard, J.R., 2003. Biological identifications through DNA barcodes. Proc. Biol. Sci. 270, 313–321. https://doi.org/10.1098/rspb.2002.2218.
Huang, J., Chen, B., 1985. Species composition and distribution of planktonic copepods in the Jiulongjiang estuarine. Taiwan Strait 4, 79–88.
Huang, J.Q., Zheng, Z., 1986. The effects of temperature and salinity on the survival of some copepods from Xiamen Harbour. Oceanol. Limnol. Sin. 17, 161–167.
Jang, M.C., Jang, P.G., Shin, K.S., Park, D.W., Jang, M., 2004. Seasonal variation of zooplankton community in Gwangyang Bay. Korean J. Environ. Biol. 22, 11–29.
Jeong, Y.S., Choo, S., Soh, H.Y., 2022. Influence of rainfall events on zooplankton community characteristics and feeding habits in estuarine–coastal environments. Front. Mar. Sci. 9, 950695. https://doi.org/10.3389/fmars.2022.950695.
Jiaqi, H., Youhuan, H., Changshou, Z., Xu, C., 1997. Distribution of zooplankton in Nanri Islands sea area of Fujian Province. Donghai Mar. Sci. 15, 46–53.
Johnson, K.P., Cruickshank, R.H., Adams, R.J., Smith, V.S., Page, R.D.M., Clayton, D.H., 2003. Dramatically elevated rate of mitochondrial substitution in lice (Insecta: Phthiraptera). Mol. Phylogen. Evol. 26, 231–242. https://doi.org/10.1016/S1055-7903(02)00342-1.
Jun, J., Kim, E., Jeon, D., Yang, J., Jeong, H.G., Jung, H., Kim, T., Eyun, S., 2024. Comparative genomic analysis of copepod humoral immunity genes with sex-biased expression in Labidocera rotunda. J. Invertebr. Pathol. 207, 108198. https://doi.org/10.1016/j.jip.2024.108198.
Kalyaanamoorthy, S., Minh, B.Q., Wong, T.K.F., Von Haeseler, A., Jermiin, L.S., 2017. ModelFinder: fast model selection for accurate phylogenetic estimates. Nat. Methods 14, 587–589. https://doi.org/10.1038/nmeth.4285.
Kang, S.Y., Moon, J.H., 2022. Distribution of water masses and characteristics of temperature inversion in the Western Seas of Jeju Island in spring. Ocean Polar Res. 44, 191–207. https://doi.org/10.4217/OPR.2022018.
Katoh, K., Misawa, K., Kuma, K., Miyata, T., 2002. MAFFT: a novel method for rapid multiple sequence alignment based on fast Fourier transform. Nucleic Acids Res. 30, 3059–3066. https://doi.org/10.1093/nar/gkf436.
Ki, J.S., Lee, K.W., Park, H.G., Chullasorn, S., Dahms, H.U., Lee, J.S., 2009. Phylogeography of the copepod *Tigriopus japonicus* along the Northwest Pacific rim. J. Plankton Res. 31, 209–221. https://doi.org/10.1093/plankt/fbn100.
Kim, K., Rho, H.K., Lee, S.H., 1991. Water masses and circulation around Cheju-Do in summer. KSO 26, 262–277.
Kozlov, A., Darriba, D., Flouri, T., Morel, B., Stamatakis, A., 2018. RAxML-NG: a fast, scalable, and user-friendly tool for maximum likelihood phylogenetic inference. Bioinform 35, 4453–4455. https://doi.org/10.1093/bioinformatics/btz305.
Kumar, M., Shukla, P., 2005. Use of PCR targeting of internal transcribed spacer regions and single-stranded conformation polymorphism analysis of sequence variation in different regions of rRNA genes in fungi for rapid diagnosis of mycotic keratitis. J. Clin. Microbiol. 43, 662–668. https://doi.org/10.1128/jcm.43.2.662-668.2005.
Lee, Y.G., Choi, J.M., Oertel, G.F., 2008. Postglacial sea-level change of the Korean Southern Sea shelf. J. Coast. Res. 118–132.
Lee, Y., Ni, G., Shin, J., Kim, T., Kern, E.M., Kim, Y., Kim, S., Chan, B., Goto, R., Nakano, T., 2021. Phylogeography of Mytilisepta virgata (Mytilidae: Bivalvia) in the northwestern Pacific: Cryptic mitochondrial lineages and mito-nuclear discordance. Mol. Phylogen. Evol. 157, 107037. https://doi.org/10.1016/j.ympev.2020.107037.
Lee, E.H., Seo, M.H., Yoon, Y.H., Choi, S.D., Soh, H.Y., 2017. Environmental factors affecting zooplankton community in Gwangyang Bay. Korean J. Environ. Biol. 35, 631–639. https://doi.org/10.11626/KJEB.2017.35.4.631.
Leigh, J.W., Bryant, D., Nakagawa, S., 2015. POPART: full-feature software for haplotype network construction. Methods Ecol. Evol. 6. https://doi.org/10.1111/2041-210X.12410.
Li, C., Sun, S., Wang, R., Wang, X., 2004. Feeding and respiration rates of a planktonic copepod (*Calanus sinicus*) oversummering in Yellow Sea Cold Bottom Waters. Mar. Biol. 145, 149–157. https://doi.org/10.1007/s00227-004-1306-x.
Lin, J., 1997. Distribution of planktonic copepods in Sansha Bay. Fujian. Mar. Sci. Bull. 16, 13–19.
Lin, J., Chen, R., 1992. Distribution of planktonic copepods in Dongshan Bay, Fujian province. Mar. Sci. Bull. 11, 41–46.
Pan, J., Cheng, F., Yu, F., Shi, Y., Sun, F., Si, G., Wei, C., Diao, X., Zhao, Y., 2021. Vertical fine-scale distribution of *Calanus sinicus* in the Yellow Sea Cold Water Mass during the over-summering process. Front. Mar. Sci. 8, 644043. https://doi.org/10.3389/fmars.2021.644043.
Pu, X.M., Sun, S., Yang, B., Ji, P., Zhang, Y.S., Zhang, F., 2004. The combined effects of temperature and food supply on *Calanus sinicus* in the southern Yellow Sea in summer. J. Plankton Res. 26, 1049–1057. https://doi.org/10.1093/plankt/fbh097.
Puvanasundram, P., Esa, Y.B., Rahim, K. a A., Amin, S.M.N., 2018. Phylogeography and population structure of *Tenualosa toli* inferred from *Cytochrome b* mitochondrial DNA fragment. J. Environ. Biol. 39, 895–906. https://doi.org/10.22438/jeb/39/5(SI)/26.
Quan, J., Lü, X.M., Zhuang, Z., Dai, J., Deng, J., Zhang, Y.P., 2001. Note: Low genetic variation of *Penaeus chinensis* as revealed by mitochondrial *COI* and *16S* rRNA gene sequences. Biochem. Genet 39, 279–284.
Rozas, J., Ferrer-Mata, A., Sánchez-Delbarrio, J.C., Guirao-Rico, S., Librado, P., Ramos-Onsins, S.E., Sánchez-Gracia, A., 2017. DnaSP 6: DNA sequence polymorphism analysis of large data sets. Mol. Biol. Evol. 34, 3299–3302. https://doi.org/10.1093/molbev/msx248.
Song, C., Choi, H., Jeon, M., Kim, E., Jeong, H., Kim, S., Kim, C., Hwang, H., Purnaningtyas, D.W., Lee, S., Eyun, S., Lee, Y., 2021. Zooplankton diversity monitoring strategy for the urban coastal region using metabarcoding analysis. Sci. Rep. 11, 24339. https://doi.org/10.1038/s41598-021-03656-3.
Song, C., Purnaningtyas, D.W., Choi, H., Jeon, D., Kim, S., Hwang, H., Kim, C., Lee, Y., Eyun, S., 2024. Do red tide events promote an increase in zooplankton biodiversity? Environ. Pollut. 361, 124880. https://doi.org/10.1016/j.envpol.2024.124880.
Uye, S., 1988. Temperature-dependent development and growth of *Calanus sinicus* (Copepoda: Calanoida) in the laboratory. Hydrobiologia 167, 285–293.
Uye, S., 2000. Why does *Calanus sinicus* prosper in the shelf ecosystem of the Northwest Pacific Ocean? ICES J. Mar. Sci. 57, 1850–1855. https://doi.org/10.1006/jmsc.2000.0965.
Väinölä, R., Vainio, J.K., Palo, J.U., 2001. Phylogeography of "glacial relict" Gammaracanthus (Crustacea, Amphipoda) from boreal lakes and the Caspian and White seas. Can. J. Fish. Aquat. Sci. 58, 2247–2257. https://doi.org/10.1139/f01-165.
Vilgalys, R., 1994. Phylogenetic implications of generic concepts in fungal taxonomy: the impact of molecular systematic studies. Mycol. Helv. 6, 73–91.
Voisin, M., Engel, C.R., Viard, F., 2005. Differential shuffling of native genetic diversity across introduced regions in a brown alga: aquaculture vs. maritime traffic effects. Proc. Natl. Acad. Sci. USA 102, 5432–5437. https://doi.org/10.1073/pnas.0501754102.
Wang, L., Wei, H., Batchelder, H.P., 2014. Individual-based modelling of *Calanus sinicus* population dynamics in the Yellow Sea. Mar. Ecol. Prog. Ser. 503, 75–97. https://doi.org/10.3354/meps10725.
Wang, S., Zhang, F., Li, Q., Zang, W., Chi, X., Tao, Z., Sun, S., 2025. Zooplankton diel vertical migration and its mediated active carbon flux in the South China Sea under the influence of mesoscale eddies. J. Plankton Res. 47, fbaf031. https://doi.org/10.1093/plankt/fbaf031.
Wang, R., Zuo, T., Wang, K., 2003. The Yellow Sea Cold Bottom Water—an oversummering site for *Calanus sinicus* (Copepoda, Crustacea). J. Plankton Res. 25, 169–183. https://doi.org/10.1093/plankt/25.2.169.
Willett, C.S., 2012. Quantifying the elevation of mitochondrial DNA evolutionary substitution rates over nuclear rates in the intertidal copepod *Tigriopus californicus*. J. Mol. Evol. 74, 310–318. https://doi.org/10.1007/s00239-012-9508-1.
Yoon, S.C., Yoon, Y.Y., 2015. Distributions of dissolved Pb and Cd in the surface water of East Sea, Korea. J. Korean Soc. Mar. Environ. Energy 18, 64–73. https://doi.org/10.7846/JKOSMEE.2015.18.2.64.
Zhang, G.T., Sun, S., Yang, B., 2007. Summer reproduction of the planktonic copepod *Calanus sinicus* in the Yellow Sea: influences of high surface temperature and cold bottom water. J. Plankton Res. 29, 179–186. https://doi.org/10.1093/plankt/fbm005.
Zhao, W., Dai, L., Chen, X., Wu, Y., Sun, Y., Zhu, L., 2022. Characteristics of zooplankton community structure and its relationship with environmental factors in the South Yellow Sea. Mar. Pollut. Bull. 176, 113471. https://doi.org/10.1016/j.marpolbul.2022.113471.